Ground Movement Analysis in Post-mining City Using MTInSAR with Help of European Ground Motion Service

C. H. Yang *, C. Stemmler, A. Müterthies

EFTAS Remote Sensing Transfer of Technology, Münster, Germany – (chia-hsiang.yang, carsten.stemmler, andreas.mueterthies)@eftas.com

KEY WORDS: MTInSAR, Soil Moisture, Post-mining Monitoring, Sentinel-1, European Ground Motion Service

ABSTRACT:

Ground movement is a critical concern for urban safety, and understanding its causes and consequences is essential. Mining of hard coal in the Ruhr area of Germany has caused long-term subsidence, leading to building damage and sinkholes in affected cities. The multi-temporal interferometric synthetic aperture radar (MTInSAR) technique has been widely adopted for estimating ground movement at millimetre-level accuracy using spaceborne SAR data. Although many European government institutes have implemented this technique for monitoring purposes, the European Ground Motion Service (EGMS) provides up-to-date ground movement products (until the end of 2020) across 31 countries. However, these products may not always meet the requirements for local use due to being untimely or missing important features. This paper demonstrates how we estimated ground movement in Ahlen, around the Ruhr area of Germany, using EGMS data as a priori and reference source. We implemented MTInSAR using Sentinel-1 data from 2018 to 2021 and compared our results with those of EGMS. Our results reveal the movement one year ahead, contain more measurement points, and cover natural areas such as cropland and bare soil. We interpreted several movement scenarios in detail, and our work highlights the benefits of EGMS as an open-source overview for local monitoring applications. We also explored the influence of soil conditions on ground movement. Our findings suggest that the overall uplift trend observed during the post-mining phase has been mitigated or even reversed, likely due to soil shrinkage resulting from drought conditions, particularly in areas with high organic soil content.

1. INTRODUCTION

Ground movement could lead to damages at buildings and infrastructures like bridges, pipelines, railways, and tunnels in a human settlement. A long-term movement of a certain size is usually caused by human activities, e.g., post-mining, tunnelling, groundwater usage, etc. Besides, a structure can deform due to other impacts. For instance, a railway bridge is deformable against thermal expansion and traffic load. For safety, terrestrial survey has been widely used to monitor hotspots or important infrastructures. This technique is regarded as an accurate benchmark but also expensive especially for a wide measurement range. In comparison, spaceborne remote sensing is more cost-effective but inflexible or rather limited in time and space. Due to its global potential, the hard- and software development keeps boosting the market growth. In practice, a monitoring scheme integrating various resources like in-situ measurement and satellite-based data has become a world trend.

Multi-temporal interferometric synthetic aperture radar (MTInSAR) (Rosen et al., 2000; Xue et al., 2020) has been widely used to estimate ground movement at millimetre level from spaceborne SAR data. This technique contains two major families: persistent scatterer interferometry (PSI) (Ferretti et al., 2001, 2011; Hooper et al., 2004, 2007) and distributed scatterer interferometry (DSI) (Goel and Adam, 2014; Lanari et al., 2004, 2007). A milestone in 2015 was the open source of Sentinel-1 data under the Copernicus Programme, which features global coverage and repeat cycle of 6 days. Since then, it has promoted many R&D and commercial projects globally at local, national, and even continental level. For example, the Ground Motion Service Germany reveals the movement map covering whole Germany for free. The movement period starts from April 2015 to December 2021. Another public service is the European Ground Motion Service (EGMS), whose movement data covers 31 European countries from February 2015 to December 2020.

The industrial coal mining, active in 19th century until 2018, in the Ruhr area (populated ≥ 5 million over 4,435 km^2), Germany has caused an extensive and continuous ground movement. Many building damages, subsidence areas, and sinkholes were reported and registered in the city management. To our knowledge, only satellite-based MTInSAR has the potential for an operational monitoring scheme across the whole area. Two pilot projects "Gemeinsames Monitoring im Alt- und Nachbergbau" (Melchers et al., 2020), contracted by the mining companies and "Proof of Concept - Monitoring von Bodenbewegungen" (Zimmermann et al., 2022) contracted by Ruhr cities have proved the concept feasible. A commercial monitoring service is then ready to operate. An innovative project BIMSAR (2021 - 2023) (https://bimsar.eftas.services/) aims to commercialize a cloud-based monitoring platform for buildings and infrastructures. The core development is to fuse MTInSAR products and BIM models for further analysis and interpretation.

This paper, as part of the work in BIMSAR, demonstrates our MTInSAR workflow of ground movement analysis with the help of EGMS. The key processing steps are described in section 2. It shows how our task benefits from EGMS as a priori and reference sources. Section 3 illustrates the experiment. The area of interest contains the post-mining city Ahlen at the edge of the Ruhr area. The Sentinel-1 data we used covers the period from 2018 to 2021. In addition to an overview, we also selected some local examples for a closer look. Finally, the main findings, conclusions, and future works are described in Section 4.

* Corresponding author

This contribution has been peer-reviewed. The double-blind peer-review was conducted on the basis of the full paper.
https://doi.org/10.5194/isprs-annals-X-1-W1-2023-739-2023 | © Author(s) 2023. CC BY 4.0 License.

2. METHODOLOGY

Our production of movement data is bundled by 5 modules (Figure 1). More details are referred to the subsections in the following. EGMS is used as a priori and reference sources. On the one hand, its accuracy in general is not comparable to the ground truth from, e.g., GPS and levelling; on the other hand, it covers numerous measurement points especially in a built-up area. Ground truth was often missing in many cases of our business. In comparison, EGMS is maintainable and accessible in all respects. A proposal would be requested or suggested between shareholders and service providers when EGMS raises the attention on a hotspot(s) of large ground movement. The MTInSAR processing will be adapted according to EGMS data. For example, an iteration interval of movement velocity can be hence determined not only to optimize the processing time but also to mitigate the risk of erroneous estimation. Our basic algorithms contain PSI and DSI, which bring accurate results for urban and natural areas, respectively. Afterwards, the movement data will be calibrated and refined to match the reality or rather reference. Here EGMS is considered as a reliable reference source while the ground truth derived from more accurate measurement is unavailable. Finally, the movement data will be packed as products under agreed formats, e.g., point cloud, vector, digital map, or print-out.

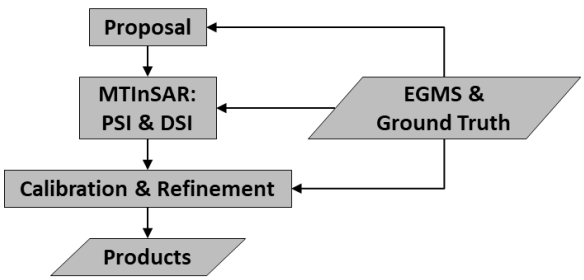

Figure 1. Production of movement data derived by MTInSAR with help of EGMS.

2.1 MTInSAR processing

The commercial and open-source softwares including ENVI, SARscape, IDL, etc. are bundled to build the main processing chain. ENVI, a specialized software of remote sensing, provides basic tools of image processing such as import, export, display, format conversion, and so on. The core algorithms of PSI and DSI are implemented in SARscape. We programmed versatile functions by IDL especially for calibration, refinement, quality control, and analysis. In addition, we also worked with GMT, Python, GDAL, SketchUp, and ArcGIS to map and analyse our product.

Nowadays, PSI (Crosetto et al., 2016; Ferretti et al., 2001, 2011) and DSI (Goel and Adam, 2014; Lanari et al., 2007), as two major MTInSAR families, haven developed into mature techniques. The accuracy of movement estimate is up to millimetre level under well-controlled conditions. We refer the readers, which are interested in the algorithms, to the relevant references cited above. PSI processes a time series of SAR images to detect target points of interest, which are characterized by coherent signals reflected from a (ground) patch of a certain size (dependent on image resolution). Here a target point can be interpreted as a measurement point. Man-made structures are therefore potential target points. Different kinds of movement are derived from these coherent signals such as cumulative time series and mean velocity. The main limitation of PSI is that the target points are rarely found in natural areas like grassland due to coherence loss. In contrast, DSI, adapted from PSI, can detect meaningful target points over natural areas. However, the accuracy of movement estimation is a bit degraded; the processing time is in general more consuming.

2.2 European ground motion service

EGMS (https://egms.land.copernicus.eu/) provides free access to ground movement from February 2015 to December 2020 across the land of 31 countries. The technical detail and quality control are described in Ferretti et al. (2021) and Steen et al. (2021), respectively. PSI algorithm is considered as the standard and mainly implemented. The main data source comes from Sentinel-1; the commercial images of high spatiotemporal resolution were also used in case of specific needs, e.g., a high-risk subsidence region. The data will be updated annually. For instance, the movement during 2021 should be available in early 2023. The point density depends on land cover and product level. This paper considers only the highest Ortho-product. The movement was calibrated into absolute vertical and horizontal components at 100 m grid (A target point covers a patch of 100 m × 100 m.).

2.3 Calibration and refinement

This module aims to correct the residual errors and fit our products towards the reality. Some important steps are summarized as follows. 1) The line-of-sight movement will be decomposed into vertical and horizontal components (Czikhardt et al., 2017). This step is crucial in case of a large-scale ground movement caused by, e.g., post-mining, groundwater usage, or tunnelling. 2) The atmospheric noise is suppressed by involving calibration data of Generic Atmospheric Correction Online Service (GACOS). 3) All movement values are so shifted that the median is anchored to 0, i.e., zero movement. Such a simple shift effectively neutralizes the systematic biases of different kind (Ferretti et al., 2021). 4) The stepwise movement series is fitted to a polynomial each. Thus, other movement forms can be derived, for example, velocity and acceleration. In addition, the effect of temporal noise and outliers can be mitigated.

3. EXPERIMENTS AND DISCUSSIONS

3.1 Background of post-mining movement in Ahlen

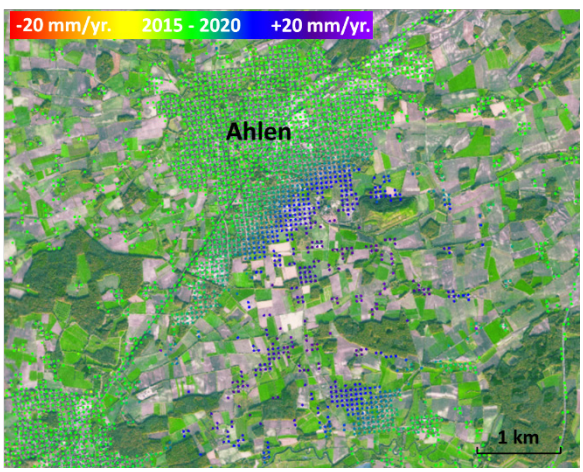

Figure 2. EMGS vertical movement map in post-mining Ahlen (51°45′48″N 7°53′28″E). Time period: February 2015 to December 2020. Positive and negative velocities, uplift and subsidence. Each target point represents the centre of a patch of 100 m × 100 m. Copyright © EGMS. All rights reserved.

The coal mining in Ahlen (Figure 2) on the edge of Ruhr area, Germany was active since 1909 and abandoned in 2000s. During the active period, the groundwater was pumped out, which together with the underground extraction of material leaded to subsidence as expected. After mine closure, the pumping stopped, so that the water level continued to raise due to precipitation and groundwater flow. Consequently, the ground uplifted as the ground layer swelled. Between 2015 and 2020, the data from EGMS exposes an area of ground uplift spanning almost 6 km × 6 km, with uplift rates reaching up to 20 mm/yr. To our knowledge, most of the residents were not informed about this uplift scenario. The consortium in BIMSAR briefed the city administration of Ahlen about the up-to-date movement up to end of 2021. The movement in 2021 was not yet added to EGMS's database. We generated our MTInSAR products by taking EGMS as reference.

3.2 Movement products

From EGMS (Figure 2), we learned two important hints to generate our movement products extended to 2021. First, the uplift concentrated to the south-east of Ahlen nearly 6 km × 6 km. Second, the velocity is up to 20 mm/yr. With this information, we then framed our parameters for the PSI- and DSI-workflows. Much of resource were thus spared without trial and error for optimized parameter settings. The Sentinel-1 data were downloaded from Copernicus Open Access Hub (https://scihub.copernicus.eu/). All deliveries were shipped as a Single Look Complex (SLC) format and then imported into our processing chain.

The key features of EGMS data and our products are compared in Table 1. Our movement period extends to 2021 and provides the local authorities up-to-date information. The point size in EGMS was resampled to 100 m × 100 m to balance the processing burden. In comparison, our PSI product takes advantage of full resolution, i.e., roughly 5 m × 15 m, so that the building movement should be more interpretable. The resolution of DSI product was downsampled to 30 m × 30 m. The reason is to minimize the errors from phase unwrapping, which directly affects the movement accuracy. The max point density (pts/km^2) is converted from the point ground size to give a more intuitive comparison. The EGMS data will be updated annually. However, the exact release date and the extended movement period were not clarified. Our products for this area in discussion can be updated within less than 72 hours. The point cloud in EGMS can be found mostly in urban areas as PSI algorithm is involved in the processing, same for our PSI product. One advantage of our DSI data is to cover both urban and natural areas. Finally, the movement of a DSI point is correlated somehow to the neighbouring ones. This is mainly caused by the spatial phase unwrapping. For example, the boundary across a subsidence and an uplift would be like a buffer or rather an overlapping area. Such an artefact is suppressed by the following modelling and filtering.

Table 1. Feature comparison of MTInSAR products

	EGMS	Our PSI	Our DSI
Movement Period	2015 - 2020	2018 - 2021	2018 - 2021
Point Ground Size	100 m × 100 m	5 m × 15 m	30 m × 30 m
Max Point Density	100 pts/km^2	13333 pts/km^2	1111 pts/km^2
Updating Time	Annually	24 - 48 Hours	48 - 72 Hours
Land Cover	Urban	Urban	Urban + Natural

The vertical movement maps of our PSI and DSI products around Ahlen are shown in Figure 3 and Figure 4. Thanks to the a priori information provided by EGMS, we received a reasonable result in our first computation. Such a cost-effectiveness benefits especially commercial projects. To be comparable, both movement data were anchored to a stable area (≈ 0 mm/yr.) chosen from EGMS as reference. Our PSI result (Figure 3) shows the same velocity pattern as seen in EGMS (Figure 2). This is a strong hint that our processing should not contain significant errors. The first noticeable feature in our DSI result (Figure 4) is a larger coverage of target points. This gives us the possibility to analyse the movement, missing in EGMS and our PSI product, in particular over the fields and vegetation covers. Various kinds of movement were subject to different reasons or mixed causes. Please note that, we did skip the thresholding on purpose to obtain a full point coverage. We explored the causes of the ground movement, if any, in the field and the potential correlation to pedology, hydrology, agriculture, etc. Our previous studies pioneered this topic and concluded some interesting findings (Yang and Müterthies, 2020, 2021). More details of our PSI and DSI-results are described by the selected examples in the following sections.

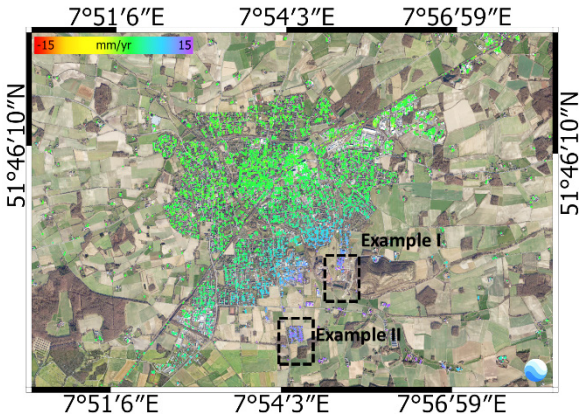

Figure 3. PSI vertical movement map in post-mining Ahlen (51°45′48″N 7°53′28″E). Velocity is scaled between -15 mm/yr. and 15 mm/yr. Time period: January 2018 to December 2021. Each target point represents the centre of a patch of 5 m × 15 m. Positive and negative velocities, uplift and subsidence. Examples will be discussed in the following sections.

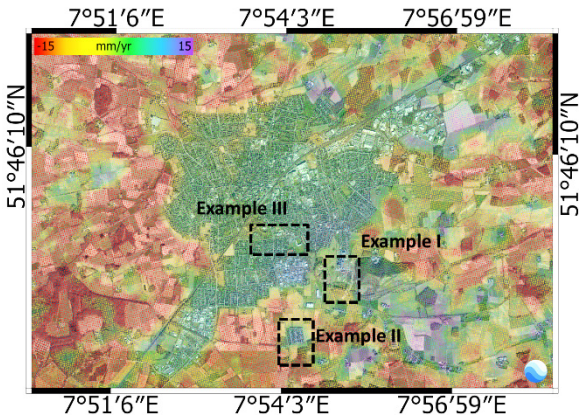

Figure 4. DSI vertical movement map in post-mining Ahlen (51°45′48″N 7°53′28″E). Velocity is scaled between -15 mm/yr. and 15 mm/yr. Time period: January 2018 to December 2021. Each target point represents the centre of a patch of 30 m × 30 m. Positive and negative velocities, uplift and subsidence. Examples will be discussed in the following sections.

The autocorrelation of PSI and DSI movement series around the built-up regions are shown in Figure 5 and Figure 6. An autocorrelation quantifies the temporal pattern of a signal series.

The closer to 1 this index is, the more relevant the movement series is. For example, a random movement is regarded as low meaningful (low autocorrelation) even it underwent a big movement at one time. In contrast, a long-term slow subsidence leads to a high autocorrelation. In PSI case (Figure 5), the ground uplift in the south-east of Ahlen is confirmed as highly relevant as expected; the others are much less important. A similar situation is also found in DSI case (Figure 6). What's more here is the movement data also cover extensive non-urban areas. Most of them are considered as a meaningful movement while they should be connected to soil property or hydrologic status.

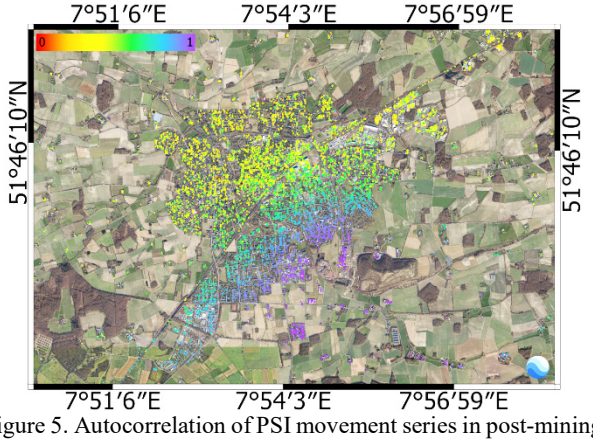

Figure 5. Autocorrelation of PSI movement series in post-mining Ahlen (51°45′48″N 7°53′28″E). Time period: January 2018 to December 2021. Each target point represents the centre of a patch of 5 m × 15 m. Towards 1 (purple), movement series more relevant.

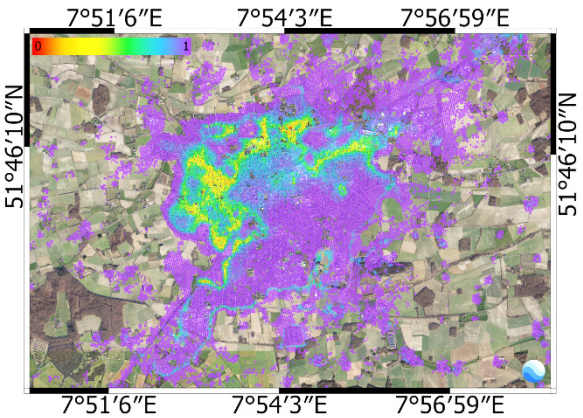

Figure 6. Autocorrelation of DSI movement series in post-mining Ahlen (51°45′48″N 7°53′28″E). Time period: January 2018 to December 2021. Each target point represents the centre of a patch of 30 m × 30 m. Towards 1 (purple), movement series more relevant.

3.3 Example I – mining campus Zeche Westfalen

Our first example considers mining campus Zeche Westfalen (Example I, Figure 3 and Figure 4), where the mining facilities and office buildings are located. Our zoom-in PSI and DSI results (Figure 7 and Figure 8) reveal that the whole campus was uplifting at around 10 mm/yr. until end of 2021. The DSI case also shows that the vegetation land on the west side outside the campus was stable. A reason could be that the uplift was offset by the soil shrinkage due to drainage (Yang and Müterthies, 2020) or by the subsidence caused by moisture change (Yang and Müterthies, 2021). In contrast, the area on the east side of the campus was uplifting.

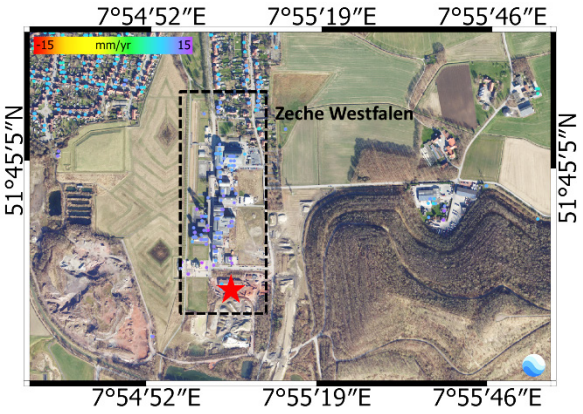

Figure 7. Zoom-in PSI result (Example I, Figure 3) around mining campus Zeche Westfalen (dotted square). Point-based analysis in Figure 9 and Figure 10: red star, namely PSI mining facility.

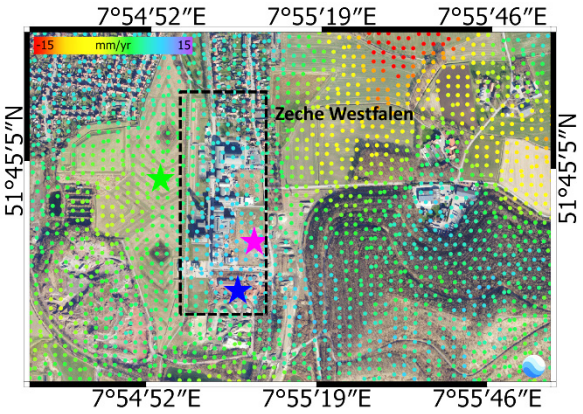

Figure 8. Zoom-in DSI result (Example I in Figure 4) around mining campus Zeche Westfalen (dotted square). Points for further analysis. Point-based analysis in Figure 9 and Figure 10: blue star, namely DSI mining facility; green star, namely DSI grass outside Campus; magenta star, namely DSI grass in campus.

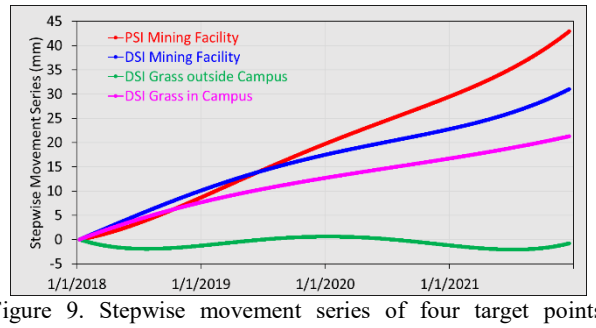

Figure 9. Stepwise movement series of four target points, selected from PSI (Figure 7) and DSI (Figure 8) results.

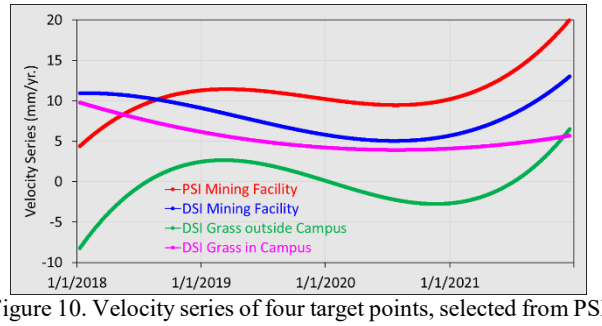

Figure 10. Velocity series of four target points, selected from PSI (Figure 7) and DSI (Figure 8) results.

This contribution has been peer-reviewed. The double-blind peer-review was conducted on the basis of the full paper.
https://doi.org/10.5194/isprs-annals-X-1-W1-2023-739-2023 | © Author(s) 2023. CC BY 4.0 License.

We selected four target points to analyse their stepwise movements (Figure 9) and velocities (Figure 10) along time. Overall, as shown in Figure 9, the grass one outside the campus remained stable without remarkable movement; the other three continued to uplift since the beginning. These phenomena just continued since the beginning of 2021. This new period was not yet covered in EGMS. Both target points of PSI and DSI on the mining facility were moving nearly the same way. The difference in the cumulative movement in four years is around 10 mm. This discrepancy is expected because these two points are 12.5 m away and represent two patches of different size (5 m × 15 m vs 30 m × 30 m). We also observe that their uplift velocities were noteworthily accelerating. The cause must be carefully investigated for building or city safety. The authority of Zeche Westfalen as the owner of the former mining campus was informed and empowered us for further investigation. In addition, a prototype of monitoring these buildings in detail will be created. For this purpose, we began to acquire a stack of VHR TerraSAR-X data (resolution up to 25 cm) together with DLR; the generation of BIM models was meanwhile in progress. We refer the interested reader to website: https://bimsar.eftas.services/.

3.4 Example II – village

Our second example focuses on a village right in the centre of the uplift area. The whole village was uplifting up to 13 mm/yr. according to our PSI and DSI results (Figure 11 and Figure 12). This sensitive information should be cautiously handled not just because of the potential building damage but also the impact on property value. We already briefed the city authority and discussed the following actions like a long-term monitoring plan. Around the village, the ground movement of the croplands is irregular and not easy to interpret. Basically, most of them shows a strong subsidence, which overlays with the uplift in the village. Our local knowledge presumes the movement signals of the cropland should be related to changes in soil moisture due to the drought from 2018 to 2020. This presumption has been proved in Yang and Müterthies (2020) and Yang and Müterthies (2021).

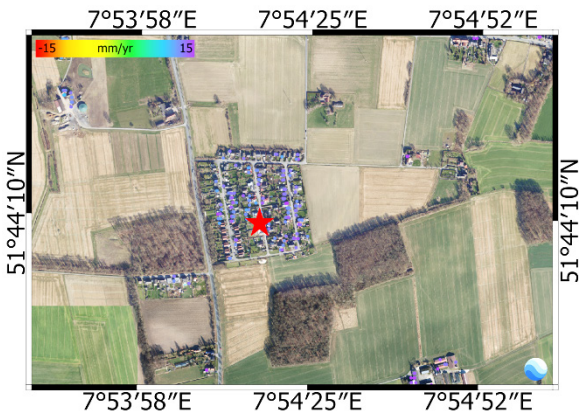

Figure 11. Zoom-in PSI result (Example II, Figure 3) around Village. Point-based analysis in Figure 13 and Figure 14: red star, namely PSI village.

Three target points were selected for time-series analysis (Figure 13 and Figure 14). The village cases from PSI and DSI were uplifting in the same way and even faster since beginning of 2021, which corresponds to the end of the drought period. The cropland point features a nominal ongoing subsidence nearly 80 mm in 4 yours. In fact, the subsidence was slowing down since middle 2020 and then turned into be uplift around 2 mm/yr. in the end of 2021. If our assumption is correct, this velocity turnaround is related to the soil moisture changes originating from the drought period 2018 to 2020.

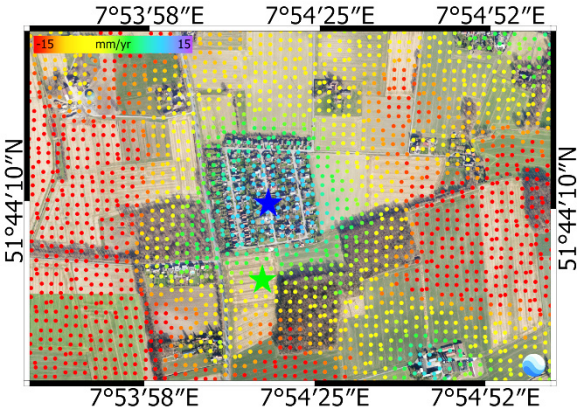

Figure 12. Zoom-in DSI result (Example II, Figure 4) around village. Point-based analysis in Figure 13 and Figure 14: blue star, namely DSI village; green star, namely DSI cropland.

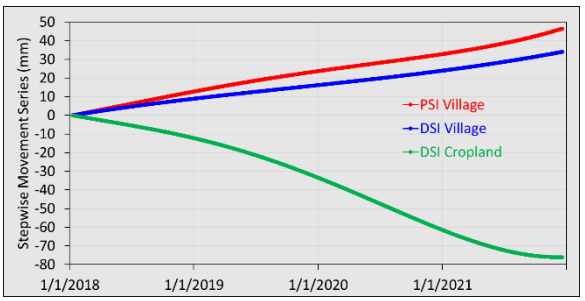

Figure 13. Stepwise movement series of three target points, selected from PSI (Figure 11) and DSI (Figure 12) results.

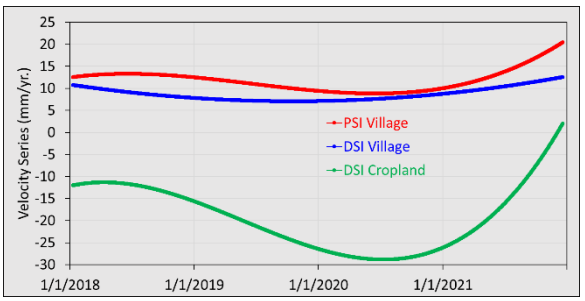

Figure 14. Velocity series of three target points, selected from PSI (Figure 11) and DSI (Figure 12) results.

3.5 Example III – bridges along river Werse

Monitoring the structural health of a bridge is crucial for a safe transportation. Here we selected 3 bridges along river Werse for further discussion (Figure 15). They are distributed across the border of ground uplift. The stepwise movement series just reflects their in-situ statuses (Figure 16). Bridge 1 was barely moving; in comparison, a continuous uplift trend can be seen for bridge 2; bridge 3 was affected by the largest uplift over 15 mm in four years. We noticed that the movement velocity for bridge 1 suddenly accelerated towards uplift since early 2021 (Figure 17). This could be an early warning for a potential structural damage in future even the movement seemed still trivial in the end of 2021. In comparison, the movement velocities for the other two bridges are stable. The movement of these bridges seemed harmless to the structural health. At least there were no accidents or visible damages being reported. However, we should always concern the safety especially for bridge 3 if the uplift is

lasting year by year. From our point of view, a long-term monitoring scheme is needed for this post-mining city.

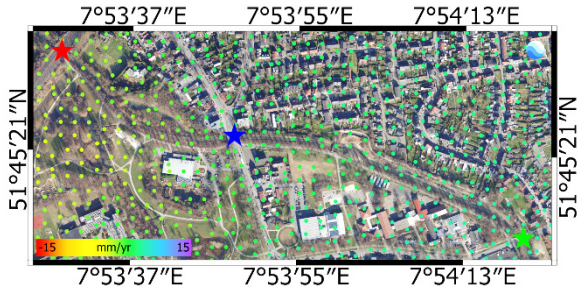

Figure 15. Zoom-in DSI result (Example III, Figure 4) across three bridges along river Werse. Bridges 1 (red star), 2 (blue star) and 3 (green star) subject to null, middle, and serious ground uplift. Point-based analysis in Figure 16 and Figure 17: red, blue, and green stars, namely, bridge 1, 2, and 3.

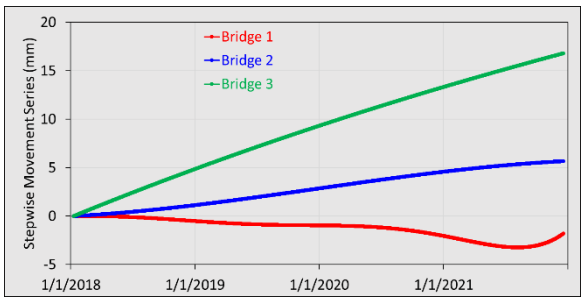

Figure 16. Stepwise movement series of three target points, selected from DSI (Figure 15) results.

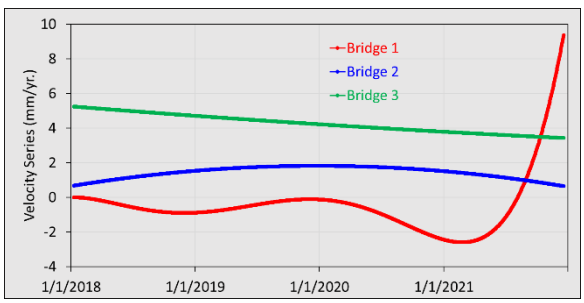

Figure 17. Velocity series of three target points, selected from DSI (Figure 15) results.

3.6 Influence of soil condition on ground movement

Normally, the MTInSAR movement will be seen as noise or error if it is not related to an actual movement such as a post-mining subsidence. Based on our experiences (Yang and Müterthies, 2020, 2021), such a nominal movement could be credited with soil moisture change or even be correlated to rainfall. For now, we focus on digging the useful signals of the movement considering soil organic content and moisture change.

Here we picked up an area in the south of Ahlen to interpret what we found from our PSI- and DSI-movement data (Figure 18 and Figure 19). The croplands situated in the middle region are located across river Lippe. This region is surrounded by several towns, where most of the PS-points are found (Figure 18). Only those PS-points in the north indicate the post-mining uplift; the others were stable without a sign of significant movement. This is what we expect as the post-mining only affects southern Ahlen (Figure 2). Given the DSI result (Figure 19), the movement scenarios in the towns are consistent with the PSI result. Moreover, the movement in the fields provides us additional information. For example, the lands along river Lippe are subject to subsidence (highlighted by red). We assume that the movement is caused by the drought-induced shrinkage of the highly organic soils in the riparian zone during the drought from 2018 to 2020. More technical details and tests are referred to Yang and Müterthies (2020, 2021).

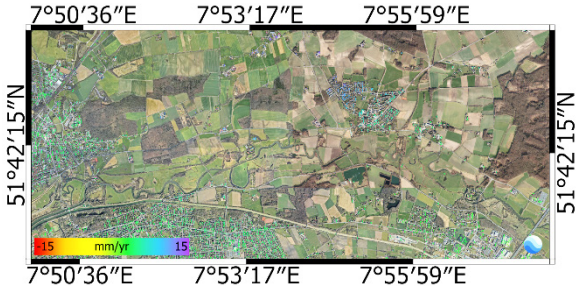

Figure 18. PSI vertical movement map in south of post-mining Ahlen (51°45′48″N 7°53′28″E). Croplands in middle region are located across river Lippe. Velocity is scaled between -15 mm/yr. and 15 mm/yr. Time period: January 2018 to December 2021. Each target point represents the centre of a patch of 5 m × 15 m. Positive and negative velocities, uplift and subsidence.

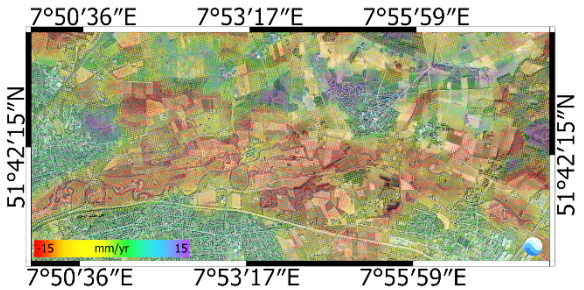

Figure 19. DSI vertical movement map in south of post-mining Ahlen (51°45′48″N 7°53′28″E). Croplands in middle region are located across river Lippe. Velocity is scaled between -15 mm/yr. and 15 mm/yr. Time period: January 2018 to December 2021. Each target point represents the centre of a patch of 5 m × 15 m. Positive and negative velocities, uplift and subsidence.

4. CONCLUSIONS AND FUTURE WORKS

We demonstrated how EGMS assisted in our project to analyse the ground movement for a post-mining city based on satellite radar data. The major contribution from EGMS is the a priori knowledge considered as open-source reference. It was used in parameter setting and quality control. Hence, we did generate our movement products in a cost-effective way. Compared with EGMS, our products are much more flexible to satisfy the requirement for a local monitoring task. For example, our movement data covers the period in 2021, which is not yet available in EGMS; we also used an additional algorithm to evaluate the movement, rarely found in EGMS, like on the vegetation cover; the density of our target points in plain is up to 133 times higher. We have briefed the city of Ahlen about the post-mining uplift. A long-term monitoring scheme is in discussion. We also explored the influence of soil conditions on ground movement. For example, the drought period from 2018 to 2020 could have resulted in the observed subsidence along river Lippe due to changes in soil moisture and/or underground water levels.

In future, we will investigate the impact of ground uplift on the buildings in Ahlen by using VHR TerraSAR-X images (resolution up to 25 cm). So far, we have collected more than 18

images and will start the processing as long as we have 20. In addition, the movement data will be fused into BIM-models of the mining campus Zeche Westfalen, which was heavily affected by the ground uplift. Afterwards, we will analyse the building movement at substructure level. Finally, we plan to conduct a comprehensive analysis of the observed ground movements to examine the impact of soil conditions and investigate potential applications, especially in the areas of pedology and hydrology.

ACKNOWLEDGEMENT

Our works were supported by project BIMSAR funded by Federal Ministry for Economic Affairs and Climate Action. We appreciate the free accesses to the data used in this study. The Sentinel-1 images were provided by Copernicus - European Union's Earth Observation Programme. The reference of ground movement was downloaded from EGMS.

BIMSAR: https://bimsar.eftas.services/

REFERENCES

Crosetto, M., Monserrat, O., Cuevas-González, M., Devanthéry, N., Crippa, B., 2016. Persistent Scatterer Interferometry: A review. ISPRS J. Photogramm. Remote Sens., 115, 78–89.

Czikhardt, R., Papco, J., Bakon, M., Liscak, P., Ondrejka, P., Zlocha, M., 2017. Ground Stability Monitoring of Undermined and Landslide Prone Areas by Means of Sentinel-1 Multi-temporal InSAR, Case Study from Slovakia. Geosci., 7(3), 1–17.

Ferretti, A., Fumagalli, A., Novali, F., Prati, C., Rocca, F., Rucci, A., 2011. A New Algorithm for Processing Interferometric Data-Stacks: SqueeSAR. IEEE Trans. Geosci. Remote Sens., 49(9), 3460–3470.

Ferretti, A., Passera, E., Capes, R., 2021. End-to-end Implementation and Operation of the European Ground Motion Service (EGMS) - Algorithm Theoretical Basis Document.

Ferretti, A., Prati, C., Rocca, F., 2001. Permanent Scatterers in SAR Interferometry. IEEE Trans. Geosci. Remote Sens., 39(1), 8–20.

Goel, K., Adam, N., 2014. A Distributed Scatterer Interferometry Approach for Precision Monitoring of Known Surface Deformation Phenomena. IEEE Trans. Geosci. Remote Sens., 52(9), 5454–5468.

Hooper, A., Segall, P., Zebker, H., 2007. Persistent Scatterer Interferometric Synthetic Aperture Radar for Crustal Deformation Analysis, with Application to Volcán Alcedo, Galápagos. J. Geophys. Res., 112(B7), B07407.

Hooper, A., Zebker, H., Segall, P., Kampes, B., 2004. A New Method for Measuring Deformation on Volcanoes and Other Natural Terrains Using InSAR Persistent Scatterers. Geophys. Res. Lett., 31(23).

Lanari, R., Casu, F., Manzo, M., Zeni, G., Berardino, P., Manunta, M., Pepe, A., 2007. An Overview of The Small Baseline Subset Algorithm: A DInSAR Technique for Surface Deformation Analysis. Pure Appl. Geophys., 164(4), 637–661.

Lanari, R., Mora, O., Manunta, M., Mallorqui, J.J., Berardino, P., Sansosti, E., 2004. A Small-baseline Approach for Investigating Deformations on Full-resolution Differential SAR Interferograms. IEEE Trans. Geosci. Remote Sens., 42(7), 1377–1386.

Melchers, C., Goerke-Mallet, P., Rudolph, T., Janzen, A., Müterthies, A., Pakzad, K., Yang, C.-H., Teuwsen, S., 2020. Abschlussbericht zum Projekt "Gemeinsames Monitoring im Alt- und Nachbergbau."

Rosen, P.A., Hensley, S., Joughin, I.R., Li, F.K., Madsen, S.N., Rodriguez, E., Goldstein, R.M., 2000. Synthetic Aperture Radar Interferometry. Proc. IEEE, 88(3), 333–382.

Steen, H., Eea, A., Andersen, H.S., 2021. End-to-end Implementation and operation of the European Ground Motion Service (EGMS) - Quality Assurance & Control Report.

Xue, F., Lv, X., Dou, F., Yun, Y., 2020. A Review of Time-Series Interferometric SAR Techniques: A Tutorial for Surface Deformation Analysis. IEEE Geosci. Remote Sens. Mag., 8(1), 22–42.

Yang, C.H., Müterthies, A., 2020. Modelling and Prediction of Precipitation and Soil Movement Based on ADInSAR. ISPRS Ann. Photogramm. Remote Sens. Spat. Inf. Sci., V-3–2020, 179–184.

Yang, C.H., Müterthies, A., 2021. Monitoring of Time-Series Soil Moisture Based on Advanced Dinsar. ISPRS Ann. Photogramm. Remote Sens. Spat. Inf. Sci., V-3–2021(3), 51–55.

Zimmermann, K., Rudolph, T., Goerke-Mallet, P., Yang, C.H., Pakzad, K., Müterthies, A., 2022. Proof of Concept - Monitoring von Bodenbewegungen.